J. Chem. Thermodynamics 68 (2014) 221–234

Contents lists available at ScienceDirect

J. Chem. Thermodynamics

journal homepage: www.elsevier.com/locate/jct

Thermophysical characterization of N-methyl-2-hydroxyethylammonium carboxilate ionic liquids

Nieves M.C. Talavera-Prieto [a], Abel G.M. Ferreira [a,*], Pedro N. Simões [a], Pedro J. Carvalho [b], Silvana Mattedi [c], João A.P. Coutinho [b]

[a] Departamento de Engenharia Química, Faculdade de Ciências e Tecnologia, Universidade de Coimbra, Pólo II, Rua Sílvio Lima, 3030-790 Coimbra, Portugal
[b] Departamento de Química, CICECO, Universidade de Aveiro, 3810-193 Aveiro, Portugal
[c] Programa de Pós-Graduação em Engenharia Química, Escola Politécnica, Universidade Federal da Bahia, Rua Aristides Novis 2, Federação, 40210-630 Salvador, Bahia, Brazil

ARTICLE INFO

Article history:
Received 29 August 2013
Received in revised form 4 September 2013
Accepted 6 September 2013
Available online 19 September 2013

Keywords:
Ionic liquids
Density
GMA equation of state
Heat capacity
Thermal stability

ABSTRACT

The thermophysical properties including density, heat capacity, thermal stability and phase behaviour of protic ionic liquids based on the N-methyl-2-hydroxyethylammonium cation, $[C_2OHC_1NH_2]^+$, with the carboxylate anions (propionate, $[C_2COO]^-$, butyrate, $[C_3COO]^-$, and pentanoate, $[C_4COO]^-$) are reported and used to evaluate structure-property relationships. The density was measured over the temperature and pressure ranges, $T = (298.15$ to $358.15)$ K and $p = (0.1$ to $25)$ MPa, respectively, with an estimated uncertainty of $\pm 0.5\ kg \cdot m^{-3}$. The pressure dependency of the density for these ionic liquids (ILs) is here presented for the first time and was correlated using the Goharshadi–Morsali–Abbaspour (GMA) equation of state, from which the isothermal compressibility, thermal expansivity, thermal pressure, and internal pressure were calculated. The experimental *PVT* data of the protic ILs were predicted by the methods of Gardas and Coutinho (GC), and Paduszyński and Domańska (PD). The thermal stability was assessed by high resolution modulated thermogravimetric analysis within the range $T = (303$ to $873)$ K. The heat capacity was measured in the temperature range $T = (286.15$ to $335.15)$ K by modulated differential scanning calorimetry with an uncertainty in the range $(1$ to $5)\ J \cdot K^{-1} \cdot mol^{-1}$. The Joback method for the prediction of ideal gas heat capacities was extended to the ILs and the corresponding states principle was employed to the subsequent calculation of liquid heat capacity based on critical properties predicted using the modified Lydersen–Joback–Reid method. The Valderrama's mass connectivity index method was also used for liquid heat capacity predictions. This series of N-methyl-2-hydroxyethylammonium was used to establish the effect of the anion alkyl chain length on the ionic liquid properties.

1. Introduction

Ionic liquids (ILs) are salts with melting points below 100 °C. They are organized in three dimensional networks of ions (cations and anions) that often possess hydrocarbon tails on their structure. In contrast with organic solvents ILs have a very low vapour pressure and can be designed as task-specific materials, for many organic reactions [1,2], liquid–liquid extractions [3,4], gas–liquid separation [5,6], heat storage [7,8], membrane-based bioseparations [9], tribologic applications [10,11] and as potential electrolytes [12]. The low vapour pressure of ILs [13] is an important property making their industrial application less risky when compared with classical solvents (*e.g.*, volatile organic compounds or VOCs). The ILs often possess low toxicities, are non-flammable materials, and have tuneable physicochemical properties such as density, viscosity, surface tension, thermal conductivity, and heat capacity. They can be divided into two main families, *viz.* aprotic ionic liquids (AILs) and protic ionic liquids (PILs). The PILs are produced by a proton transfer on stoichiometric acid-base Brønsted reaction and their main difference, compared to AILs, is the presence of at least a proton which is/are able to promote extensive hydrogen bonding [14]. To date, AILs have received greater attention than PILs, but recently there has been an increasing interest in PILs. Their protic nature is determinant in a number of uses including biological applications [15], organic synthesis [16–18], chromatography [19], as electrolytes for polymer membrane fuel cells [20], as reactants in biodiesel production [21], and as propellant or explosives [22,23]. The first PIL was hydroxyethylammonium nitrate $[C_2OHNH_3][NO_3]$ and was reported in 1888 [24] and one of the most studied is ethylammonium nitrate $[C_2NH_3][NO_3]$ first reported in 1914 [25] which has many similarities with water, including high polarity and the ability to form a hydrogen bonded network and promoting amphiphiles self-assembly [26–31]. Experimental studies for thermophysical properties of ILs have been reported for imidazolium, pyridinium and for some

* Corresponding author. Tel.: +351 239 798 729; fax: +351 239 798 703.
E-mail addresses: fabel7@gmail.com, abel@eq.uc.pt (Abel G.M. Ferreira).

0021-9614/$ - see front matter © 2013 Elsevier Ltd. All rights reserved.
http://dx.doi.org/10.1016/j.jct.2013.09.010

ammonium based ILs which are based in primary ammine cations of the form R_4N. The alkanolammonium ILs are protic ionic liquids with a huge potential in a variety of industrial fields. Alkanolamines soaps, PILs formed by the reaction between an alkanolammonium and fatty acids, are actually used in the formulation of industrial and hand-cleaners, cosmetic creams, aerosols and shave foams due to their emulsifier, and detergent ability in oil-in-water emulsions [32–35]. The monoethanolamine oleate [36] is widely used in the pharmaceutical industry as sclerosant agent [37–40].

Among other advantages, these PILs have low cost of preparation, simple synthesis and purification [41,42] as well as a very low toxicity. The degradability of this kind of PILs has been verified [43]. Despite the well recognized fundamental and practical significance of this PILs family, their fundamental thermophysical properties are either scarce or absent. A few studies made on the structure-property binomial can be summarized as follows. Greaves *et al.* [44] studied the phase behaviour of hydroxyethylammonium cation with carboxylates, nitrate and sulphate anions. Belieres and Angel [45] studied the phase transition temperatures, thermogravimetric analysis (TGA), electric conductivity, density and viscosity of hydroxyethylammonium formate, nitrate, tetrafluoroborate and triflate. The density and the viscosity were measured by Kurnia *et al.* [41] for hydroxyethylammonium and bis-(hydroxyethyl)ammonium cations with acetate and lactate anions. These properties plus the speed of sound and electrical conductivity were measured by Iglesias *et al.* [42] for 2-hydroxyethylammonium, bis(2-hydroxyethyl)ammonium, and tris(2-hydroxyethyl)ammonium cations with pentanoate anion. Experimental data on density, viscosity, speed of sound and refractive index as well as IR and NMR spectra were reported by Àlvarez *et al.* [46] for N-methyl-2-hydroxyethylammonium cation with various carboxylates (formate, acetate, propionate, butyrate, isobutyrate and pentanoate). Pinkert *et al.* [47], presented density, viscosity and electrical conductivity data for 2-hydroxyethylammonium, 3-hydroxypropylammonium, bis(2-hydroxyethyl)ammonium, and tris(2-hydroxyethyl)ammonium cations combined with formate, acetate and malonate anions. The data on thermal properties are scarce. The heat capacity has been measured by Domanska and Bogel-Lukasik [48] for *N*-alkyl-(2-hydroxyethyl)-dimethylammonium ($N = 2, 3, 6$) bromide and Mahrova *et al.* [49] who made measurements for 2-hydroxyethyl-N,N,N-alkylammonium with sulfonates and sulphates.

The aim of this study is to obtain significant data on fundamental thermophysical properties and information on thermal stability of *N*-methyl 2-hydroxyethylammonium PILs with propionate, butyrate and pentanoate anions. The thermophysical properties are the density as a function of temperature, pressure and the heat capacity. The density and its pressure-temperature dependency (*PVT* behaviour) can be considered as fundamental data for developing equations of state, which are one of the main tools used for thermophysical properties prediction for process design purposes, and solution theories of ILs. Moreover the derived properties from density as the thermomechanical coefficients (thermal expansivity, isothermal compressibility, and internal pressure) provide useful information on IL structure and molecular interactions. The volumetric behaviour of ILs are described here in terms of the Goharshadi–Morsali–Abbaspour equation of state (GMA EoS) which has been developed and found to be valid for polar, non-polar, and H-bonded fluids [50]. The experimental *PVT* data of the PILs are described by the predictive methods of Gardas and Coutinho (GC) [51] and Paduszyński and Domańska (PD) [52].

Experimental data for heat capacity of PILs are still scarce and limited to alkanolammonium PILs. More data and better understanding of heat capacity are needed for the "design" of PILs for specific applications. Moreover when experimentally measured values are not available, the theoretical or empirical methods must be used for their evaluation if the heat capacity is within acceptable limiting values defined by design specifications. The predictive methods are thus required and are an attractive way of obtaining data to make faster progress on modelling, simulation and design of process involving ILs. To date, some predictive models of heat capacity by group contribution methods (GCM) have been reported for ILs [53]. Coutinho *et al.* [53,54] developed a method to estimate the heat capacity of ILs based on experimental data collected from the literature applicable to imidazolium, pyridinium and pirrolidinium-based ILs. Another way to estimate the heat capacity of ILs is the use the Joback method for perfect gas heat capacity and the subsequent use of the principle of corresponding states to calculate the liquid heat capacity. In this approach the modified Lydersen–Joback–Reid method developed by Valderrama and Rojas [55] is used to predict the critical properties of ILs. Recently a predictive method based on the mass connectivity index [56] was presented by Valderrama *et al.* [57]. In this work, we report the results of heat capacity measurements using modulated differential scanning calorimetry for the *N*-methyl 2-hydroxyethylammonium PILs with propionate, butyrate and pentanoate anions. The experimental results of this work are used to test the predictive models mentioned. By combining the results obtained herein and reliable literature data, the molar heat capacity data of *N*-alkyl-2-hydroxyethylammonium PILs was correlated with the molar volume over wide temperature ranges.

2. Experimental

2.1. Preparation of the protic ionic liquids

The 2-methylaminoethanol was obtained from Aldrich at 0.99 mass fraction purity and the organic acid was obtained from Sigma with mass fraction purity greater than 0.995. These components were used as received. The PILs used in this work were prepared from stoichiometric quantities of the 2-methylaminoethanol and the organic acids (propionic, butyric and pentanoic) using the methodology detailed in Alvarez *et al.* [46].

The amine was placed in a triple necked glass flask equipped with a reflux condenser, a PT-100 temperature sensor for controlling temperature and a dropping funnel. The flask was mounted in an ice bath. The organic acid was added drop wise to the flask while stirring with a magnetic bar at a rate to maintain the reaction temperature below 283.15 K, since the reaction is exothermic, strong agitation (*ca.* 450 rpm) was applied in order to improve the contact between the reactants allowing the reaction to be completed. Stirring was carried for 24 h at room temperature in order to obtain a final viscous liquid. The reaction is a simple Brønsted acid–base neutralization forming an ionic liquid.

Before each use, the ILs samples were washed several times using suitable solvents to ensure removal of any remaining starting materials. The ionic liquid was further dried under low vacuum (1 Pa) and a small distilled portion of the IL, rich in water and volatile compounds was discharged. Then, under high vacuum (10^{-4} Pa) the IL was fully distilled and the distillate purity checked by ^{1}H NMR and ^{13}C NMR. The final water content was determined with a Metrohm 831 Karl Fisher coulometer indicating a water mass fraction lower than $3 \cdot 10^{-4}$. Table 1 summarizes relevant information on sample material purities.

2.2. Experimental procedure

Experimental densities of the *N*-methyl-2-hydroxyethylammonium ILs carboxylic acid anions were measured using an Anton Paar DMA 60 digital vibrating tube densimeter, with a DMA 512P measuring cell in the temperature and pressure ranges

TABLE 1
Provenance and purity of the synthesis materials and ionic liquids.

Chemical	Supplier (CAS N)	Sample purity[a]	
		Mass fraction as received	Mass fraction water content
2-methylaminoethanol	Sigma–Aldrich (109-83-1)	0.99	
Propanoic acid	Sigma–Aldrich (79-09-4)	>0.995	
Butanoic acid	Sigma–Aldrich (107-92-6)	>0.995	
Pentanoic acid	Sigma–Aldrich (109-52-4)	>0.995	
$[C_2OHC_1NH_2][C_2COO]$		>0.99	$3 \cdot 10^{-4}$
$[C_2OHC_1NH_2][C_3COO]$		>0.99	$3 \cdot 10^{-4}$
$[C_2OHC_1NH_2][C_4COO]$		>0.99	$3 \cdot 10^{-4}$

[a] The ILs were fully distilled under high vacuum (10^{-4} Pa) and the distillate mass fraction purity checked by ^{1}H NMR and ^{13}C NMR is greater than 0.99. The final water content was determined with a Metrohm 831 Karl Fisher coulometer.

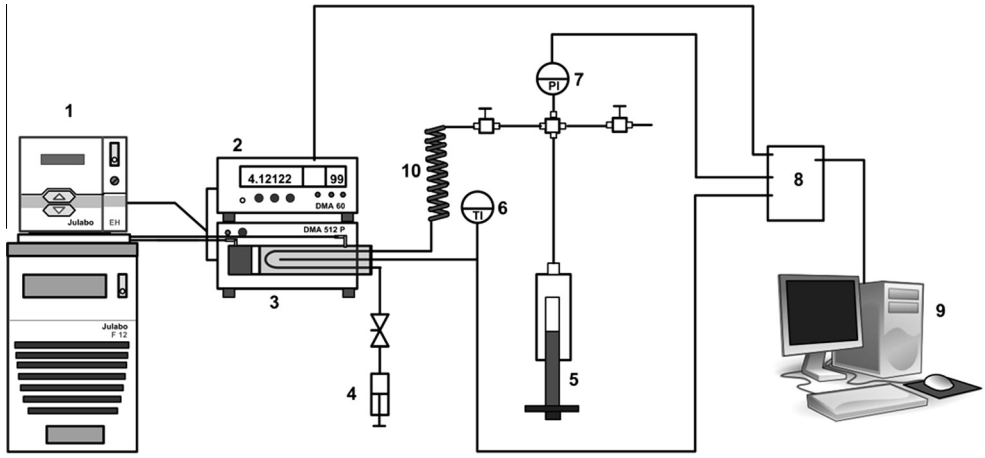

FIGURE 1. Experimental setup for the measurement of liquid densities at high pressures: 1, Julabo FP-50 thermostatic bath; 2, DMA 60 (Anton Paar) device for measuring the period of oscillation; 3, measuring cell DMA 512P (Anton Paar); 4, syringe for sample introduction; 5, pressure generator model HIP 50-6-15; 6, PT probe; 7, pressure transducer WIKA, S-10; 8, NI PCI-8220 data acquisition board; 9, PC; 10, buffer.

T = (293.15 to 343.15) K and p = (0.1 to 25.0) MPa, respectively. Figure 1 shows schematically the installation of the DMA 512P cell and the peripheral equipment used. The temperature in the vibrating tube cell was measured with a platinum resistance probe which has a temperature uncertainty of ±0.01 K. A Julabo F12-ED thermostatic bath with ethylene glycol as circulating fluid was used in the thermostat circuit of the measuring cell which was held constant to ±0.01 K. The required pressure was generated and controlled with a Pressure Generator model 50-6-15, High Pressure Equipment Co., using acetone as hydraulic fluid. The diameter of the metallic tube was $1.59 \cdot 10^{-3}$ m, and the buffer is more than 1 m in length which guarantees the inexistence of diffusion of the hydraulic liquid in the liquid contained in densimeter cell. Pressures were measured with a pressure transducer (Wika Transmitter S-10, WIKA Alexander Wiegand GmbH & Co.) with a maximum uncertainty of 0.03 MPa. An NI PCI-6220 data acquisition board (DAQ) from National Instruments (NI) was used for the real time registration of values of period, temperature, and pressure. For this task, a Labview application was developed. Modules of temperature (NI SCC-FT01) and pressure (NI SCC-CI20) were installed into a NI SC-2345 carrier and connected to the DAQ board. The calibration of the vibrating tube densimeter was made by the method proposed by Niesen *et al.* [58]. The calibration details for this method can be found elsewhere [59]. The Niesen equation is

$$\rho(T,p,\tau) = \left[\frac{\tau^2(T,p)(A_1 + A_2T + A_3T^2)}{\tau^2(T_0, p_0 = 0)}\right] + A_4 + A_5T + A_6p, \qquad (1)$$

where $\rho(T, p)$ and $\tau(T, p)$ are, respectively, the density and the vibration period which are both function of temperature (T) and pressure (p). In this work, the measured period at vacuum conditions $\tau(T_0 = 318.15$ K, $p_0 = 0.1$ MPa) = 3886665 μs was used. Water and dichloromethane were used as calibrating fluids. The standard values given by National Institute of Science and Technology (NIST) in the range of temperature 293.15 K to 393.15 K and pressures from 0.1 MPa up to 35 MPa were used. For water, the density data from NIST are specified with an uncertainty of 0.001% at pressures up to 10 MPa rising at higher pressures in the temperature range of this work but always less than 0.1% [60]. For dichlorometane, the data obtained in our previous work [61] were used. The uncertainty on density in these data is 0.06%. The fitting of equation (1) to (pVT) data of water and dichloromethane gives A_1 = 10120.04 kg · m^{-3}, A_2 = -3.3837 kg · m^{-3} · K^{-1}, $A_3 = 2.22565 \cdot 10^{-4}$ kg · m^{-3} · K^{-2}, A_4 = -9356.95 kg · m^{-3}, A_5 = 0.91099 kg · m^{-3} · K^{-1} and $A_6 = -1.0853 \cdot 10^{-1}$ kg · m^{-3} · MPa^{-1} with a standard deviation of the fitting σ = ±0.8 kg · m^{-3}. The overall accuracy of the vibrating densimeter, estimated taking into account the influence of uncertainties in temperature, pressure, period of oscillations (six-digit frequency counter), viscosity and density data of the calibrating fluids is of the order (perhaps less than) ±1.0 kg · m^{-3}. Taking into account at least four values of the period of oscillation at a given (T, p) state the precision of the measurements was of the order of ±0.1 kg · m^{-3}.

The influence of the viscosity on the density uncertainty (damping effects on the vibrating tube) was evaluated by us before in a study conducted on phosphonium–based ILs [62]. We have concluded that the uncertainties expected for density due to viscosity

of the ionic liquids falls in the interval 0.3 kg · m^{-3} to 0.5 kg · m^{-3} within the range T = (273.15 to 328.15) K. For temperatures higher than 328.15 K, we expect that uncertainties do not vary from these values.

Heat capacity measurements were carried out using a modulated differential scanning calorimeter (MDSC) equipment from TA Instruments (Q100 model). The heat flow and heat capacity were calibrated at 2 K · min^{-1} using, respectively, indium and sapphire standards. A modulation period of ~120 s, and a temperature amplitude of ±0.53 K were employed. A dry nitrogen purge flow of 50 mL · min^{-1} was applied in the calibration and measurements. It should be mentioned that great care was taken to avoid the contact of the sample with moisture during transportation. The temperature and relative humidity in the room where the experiments were carried out were under tight control. The samples were analyzed in aluminium pans with an ordinary pressed aluminium lid, in which a small hole (*ca.* <0.5 mm) was made, were submitted to a program in the TGA apparatus to contribute for the elimination of possible traces of moisture. The procedure consisted in heating the set pan/lid/sample up to T = (313-323) K (see TGA results below), an isothermal for 15 min, and an equilibration at 298 K. The sample mass observed at this stage was then used as input in the subsequent MDSC run for measuring the heat capacity. Sample masses of *ca.* 9 to 11 mg were used in the measurements.

The thermal stability of the ILs was studied by Hi-Res-MTGA, by using a TA Instruments Q500 thermogravimetric analyzer (thermobalance sensitivity: 0.1 μg). The temperature calibration was performed over the temperature range (298–1273) K by measuring the Curie point of the nickel standard, and using open platinum crucibles and a dry nitrogen purge flow of 100 cm^3 · min^{-1}. This procedure was performed at the heating rate used throughout the experimental work ($\phi = 2$ K · min^{-1}). A dynamic rate mode was used under a (maximum) heating rate of 2 K · min^{-1}, a modulation period of 200 s, and temperature amplitude of ±5 K. Sample masses of *ca.* (50–55) mg were used in the measurements.

3. Results and discussion

3.1. Density

Figure 2 shows the density as function of pressure for isothermal conditions (the experimental density data for the three ILs are reported in table S1, as supplementary information). A comparison of our values with the data measured by Àlvarez *et al.* [46] at temperatures in the range T = (278.15 to 338.15) K and atmospheric pressure is presented in figure 3. Theses authors have used a DSA-5000 digital vibrating tube densimeter (Anton Parr, Austria) with an uncertainty of ±0.1 kg · m^{-3}. It can be seen that our measured values presents a systematic deviation towards lower values. The deviations between the two sets of values can be summarized as follows: for the [$C_2OHC_1NH_2$][C_2COO] the deviations are in the range −0.5% to −0.4% at temperature limits (338.15 K, 298.15 K), for [$C_2OHC_1NH_2$][C_3COO], the deviations range from −0.4% to −0.3% and for the [$C_2OHC_1NH_2$][C_4COO] the deviations are in the range −0.7% to −0.5%.

3.1.1. Modelling and prediction

In the present work, we have used the GMA EoS to correlate the density at various temperatures and pressures. The GMA EoS is given as [50]:

$$(2z-1)V_m^3 = A(T) + B(T)\,\rho_m, \tag{2}$$

where z, V_m, and ρ_m are the compressibility factor, molar volume, and mass density, respectively. Under isothermal conditions, the quantity $(2z-1)V_m^3$ as a function of molar density gives a straight line with intercept $A(T)$ and the slope $B(T)$. The temperature dependencies of the parameters $A(T)$ and $B(T)$ are given by the equations [50]:

$$A(T) = A_0 - \frac{2A_1}{RT} + \frac{2A_2 \ln T}{R}, \tag{3}$$

$$B(T) = B_0 - \frac{2B_1}{RT} + \frac{2B_2 \ln T}{R}, \tag{4}$$

where A_0–A_2 and B_0–B_2 are the fitting parameters, and R is the gas constant. They were estimated by fitting equation (2) to data through the Lavenberg-Marquardt method. Table 2 summarizes the molar mass, M, the temperature and pressure range of density measurements, the coefficients A_0–A_2 and B_0–B_2, the standard deviation, , correlation coefficient, R^2, and number of data points, N_p used in the fitting. Figure 4 shows the results for the PILs clearly showing that the linearity holds at different temperatures. The density of the liquid at different temperatures and pressures was calculated using GMA EoS in the following form:

$$B(T)\,\rho_m^5 + A(T)\,\rho_m^4 + \rho_m - 2p/RT = 0. \tag{5}$$

The straight lines calculated from equations (2) to (4) with the parameters given in table 2 are plotted in figure 4. It can be concluded that equation (2) is quite adequate for the analytical representation of (p, ρ, T) data. The ability of GMA EoS to reproduce the density data at different temperatures and pressures may be quantitatively evaluated from the absolute average deviation (*AAD%*) which is defined as

$$\mathrm{AAD\%} = 100\sum_{i=1}^{Np}|1 - \rho_{calc}/\rho_{exp}|_i/N_p. \tag{6}$$

Using equation (5) for the calculation of the density we have obtained *AAD%* values less than 0.004% confirming that the GMA EoS correlates the experimental density data with a high degree of accuracy. The comparison of the experimental data and the calculated values of density from equation (5) as a function of the temperature and of the pressure is made graphically in figure 5 for [$C_2OHC_1NH_2$][C_2COO]. It can be observed that the GMA EoS correlates the data of this work with deviations in the range 0.005%, *i.e.*, less than 0.1 kg · m^{-3}. Equivalent comparisons were made for [$C_2OHC_1NH_2$][C_3COO] and [$C_2OHC_1NH_2$][C_4COO] with similar results.

Some important thermomechanical properties can be derived from GMA equation of state such as the isobaric expansivity, α_p = - $(1/\rho)(\partial\rho/\partial T)_p$, the isothermal compressibility, $k_T = (1/\rho)(\partial\rho/\partial p)_T$, and the internal pressure $p_i = (\partial U/\partial V)_T$, where U is the internal energy. The following equations are obtained [50]:

$$\alpha_p = \frac{(2B_1 + 2B_2T)\rho_m^5 + (2A_1 + 2A_2T)\rho_m^4 + 2p}{5\rho_m^5(RT^2B_0 - 2B_1T + 2B_2T^2\ln T) + 4\rho_m^4(RT^2A_0 - 2A_1T + 2A_2T^2\ln T) + RT^2\rho_m}, \tag{7}$$

$$k_T = \frac{2}{\rho_m RT + 5\rho_m^5(RTB_0 - 2B_1 + 2B_2T\ln T) + 4\rho_m^4(RTA_0 - 2A_1 + 2A_2T\ln T)}, \tag{8}$$

$$p_i = (B_1 + B_2T)\rho_m^5 + (A_1 + A_2T)\rho_m^4. \tag{9}$$

The thermal pressure coefficient, γ_V, may be calculated as $\gamma_V = \alpha_P/k_T$. On the basis of the thermomechanical coefficients, the internal pressure p_i can be calculated according to the relationship

$$p_i = (\partial U/\partial V)_T = T(\partial p/\partial T)_V - p = T\cdot\gamma_V - p. \tag{10}$$

The thermomechanical coefficients for [$C_2OHC_1NH_2$] ILs are plotted in figure 6 and their values at the temperature and pressure ranges of the measurements are given as supplementary material (see tables S2 to S4). Figure 6(a) shows that the (p, T) behaviour of α_p here given for [$C_2OHC_1NH_2$][C_2COO] is consistent with the observed, *i. e.* $_p$ increases with the temperature at a fixed pressure.

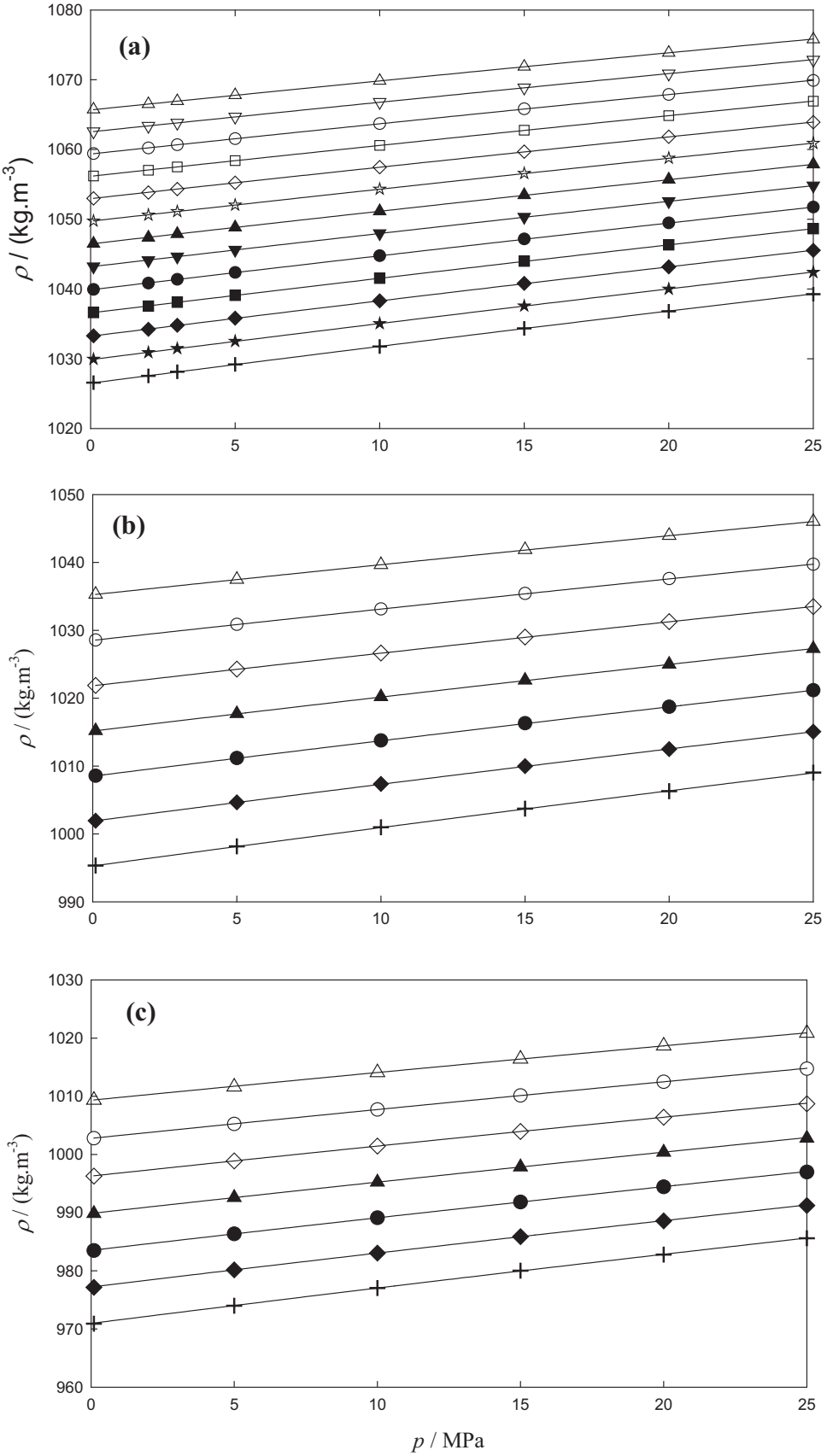

FIGURE 2. Isotherms of the density for the *N*-methyl-2-hydroxyethylammonium carboxylic ILs: (a) $[C_2OHC_1NH_2][C_2COO]$; (b) $[C_2OHC_1NH_2][C_3COO]$; (c) $[C_2OHC_1NH_2][C_4COO]$. Legend: experimental data of this work: Δ, T = 298.15 K; , 303.15 K; ○, 308.15 K; □, 313.15 K; ◇, 318.15 K; ☆, 323.15 K; ▲, 328.15 K; ▼, 333.15 K; ●, 338.15 K; ■, 343.15 K; ♦, 348.15 K; ★, 353.15 K; +, 358.15 K. Full curves calculated from GMA EoS equation.

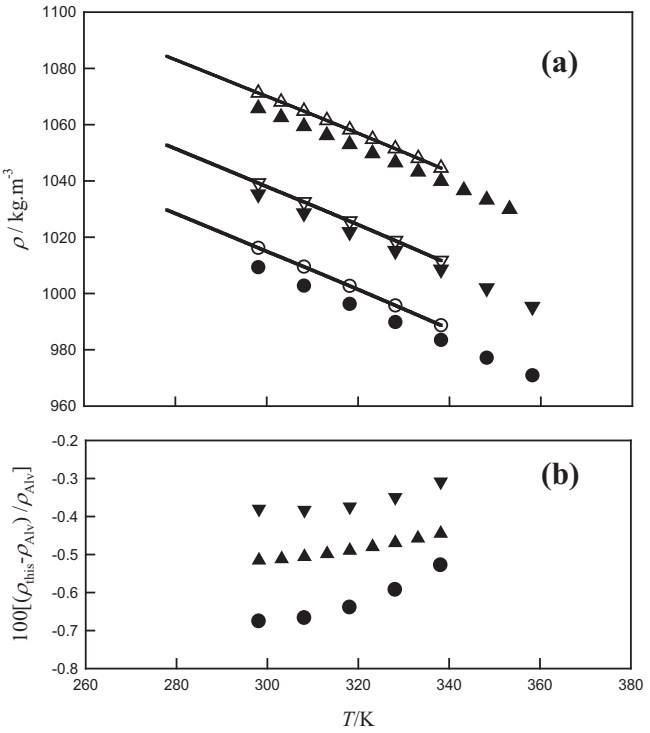

FIGURE 3. Comparison of the densities of this work at atmospheric pressure as functions of temperature with the data from Álvarez *et al.* [46]. Legend: ▲, $[C_2OHC_1NH_2][C_2COO]$; ▼, $[C_2OHC_1NH_2][C_3COO]$; ●, $[C_2OHC_1NH_2][C_4COO]$. The corresponding open symbols refer to the data due to Àlvarez *et al.*, and the continuous lines correspond to 241 experimental values presented by the authors for the tree PILs. The ρ_{this} and ρ_{Alv} correspond to the density measured in this study and by Alvarez *et al.*, respectively.

This behaviour is contrary to that which has been observed for some other ILs. From figure 6(a), it can be seen that α_p decreases with the increase of the pressure for all the isotherms as expected. Some small deviations from the expected behaviour is observed for $[C_2OHC_1NH_2][C_3COO]$ and $[C_2OHC_1NH_2][C_4COO]$. For the former α_p is almost constant with temperature for a given pressure, whereas for the later a small decrease with temperature is observed. As a whole, the PILs studied show values of α_p in the interval (5.5 to 6.6) 10^{-4} K^{-1} over the (*T*,*p*) ranges investigated. With respect to k_T, the observed behaviour on the (*p*,*T*) variables is the expected (see figure 6(b)), *i.e.*, k_T increases with the temperature for isobaric conditions and the values decrease with pressure for isothermal conditions. The minimum values are of the order 0.4 MPa^{-1}, while the maximum values are in the range (0.5 to 0.6) MPa^{-1}, and k_T increases in the order $[C_2OHC_1NH_2][C_2COO] < [C_2OHC_1NH_2][C_3COO] < [C_2OHC_1NH_2][C_4COO]$.

Although rarely used in investigations of ILs, the internal pressure p_i provides a useful basis for understanding the nature of molecular interactions in the liquid state. As the internal pressure is related to the isothermal change of entropy per unit volume it is a macroscopic property used for estimating the cohesion of liquids reflecting molecular ordering. On the other hand, the internal pressure is a measure of the change in internal energy of a liquid as it experiences a small isothermal expansion. For each of the PILs studied here, p_i is little sensitive to the variation with pressure and temperature. An isothermal decrease with pressure is always observed but with the temperature the behavior is variable depending on the nature of PIL. This situation is due to the small range of variation of γ_V with temperature and pressure. The internal pressure reaches its minimum value (p_i = 340 MPa) for $[C_2OHC_1NH_2][C_4COO]$ (at T = 358 K, p = 25 MPa) and the maximum (p_i = 451 MPa) for $[C_2OHC_1NH_2][C_2COO]$ (at T = 343 K, p = 0.1 MPa). Despite the small changes in p_i, this property increases in the following the order, $[C_2OHC_1NH_2][C_2COO] > [C_2OHC_1NH_2][C_3COO] > [C_2OHC_1NH_2][C_4COO]$. The values of the internal pressure of $[C_2OHC_1NH_2][C_2COO]$ are given as function of pressure in graphic form in figure 6(d) for several isotherms, T = (298.15 to 358.15) K at 10 K increments.

We have selected two widely applied models to predict (*p V T*) data: The Gardas and Coutinho [51] and Paduszynki and Domanska [52] models. In the first, the volumes of ions at the reference temperature (298.15 K) and pressure (0.1 MPa) are used. These volumes are calculated by means of the Ye and Shreeve procedure [63] or, if available, taken directly from the literature. The influence of temperature and pressure on the molar volume is accounted for by three universal (*i.e.*, independent of IL) coefficients found by fitting the model equation to experimental values. The authors assumed linear dependence of molar volume on temperature and pressure. The database used to obtain the coefficients included about 1500 experimental density data points for 23 ILs covering the temperature and pressure ranges of T = (293-393) K and p = (0.1 to 100) MPa. The average absolute relative deviation (AAD%) between calculated and experimental densities ranges from 0.45% to 1.57% depending on the cation of IL (imidazolium, pyridinium, pyrrolidinium, or phosphonium). The pure component density is estimated according to equation [51]

$$\rho = \frac{M}{NV(a + bT + cp)}, \tag{11}$$

TABLE 2
Fitting parameters of GMA EoS correlation applied to the experimental (P, ρ, T) data of N-methyl-2-hydroxyethylammonium carboxylic PILs. The temperature and pressure ranges (T_{min},T_{max},p_{min},p_{max}), standard deviation (σ), correlation coefficient (R^2), and number of data points (N_p) are given.

	GMA Eos, equation (3)		
	$[C_2OHC_1NH_2][C_2COO]$	$[C_2OHC_1NH_2][C_3COO]$	$[C_2OHC_1NH_2][C_4COO]$
M/(g · mol^{-1})	149.188	163.215	177.241
A_0/(dm^9 · mol^{-3})	3.91453 ± 0.6815	3.8250 ± 1.5642	2.96614 ± 3.7300
A_1/(MPa · dm^{12} · mol^{-2})	2.23699 ± 0.1377	2.92287 ± 0.3154	3.60261 ± 0.7509
A_2/(MPa · dm^{12} · mol^{-2})	$-2.1177 \cdot 10^{-3} \pm 4.1665 \cdot 10^{-4}$	$-1.9189 \cdot 10^{-3} \pm 0.001$	$-1.2243 \cdot 10^{-3} \pm 0.0023$
B_0/(dm^{12} · mol^{-4})	−0.46281 ± 0.0964	−0.32108 ± 0.2491	$-7.3483 \cdot 10^{-3} \pm 0.6615$
B_1/(MPa · dm^{15} · mol^{-3})	−0.27710 ± 0.01944	−0.37153 ± 0.0501	−0.47982 ± 0.1329
B_2/(MPa · dm^{15} · mol^{-3})	$2.5524 \cdot 10^{-4} \pm 5.8926 \cdot 10^{-5}$	$1.4891 \cdot 10^{-4} \pm 0.0002$	$-7.04341 \cdot 10^{-5} \pm 0.0004$
T_{min}/K	298.15	298.15	298.15
T_{max}/K	358.15	358.15	358.15
p_{min}/ MPa	0.10	0.10	0.10
p_{max}/MPa	25.0	25.0	25.0
σ/(dm^9 · mol^{-3})	$1.5 \cdot 10^{-5}$	$2.6 \cdot 10^{-5}$	$6.3 \cdot 10^{-5}$
R^2	1.000	1.000	1.000
N_p	104	42	42
AAD/%	0.0018	0.0027	0.0037

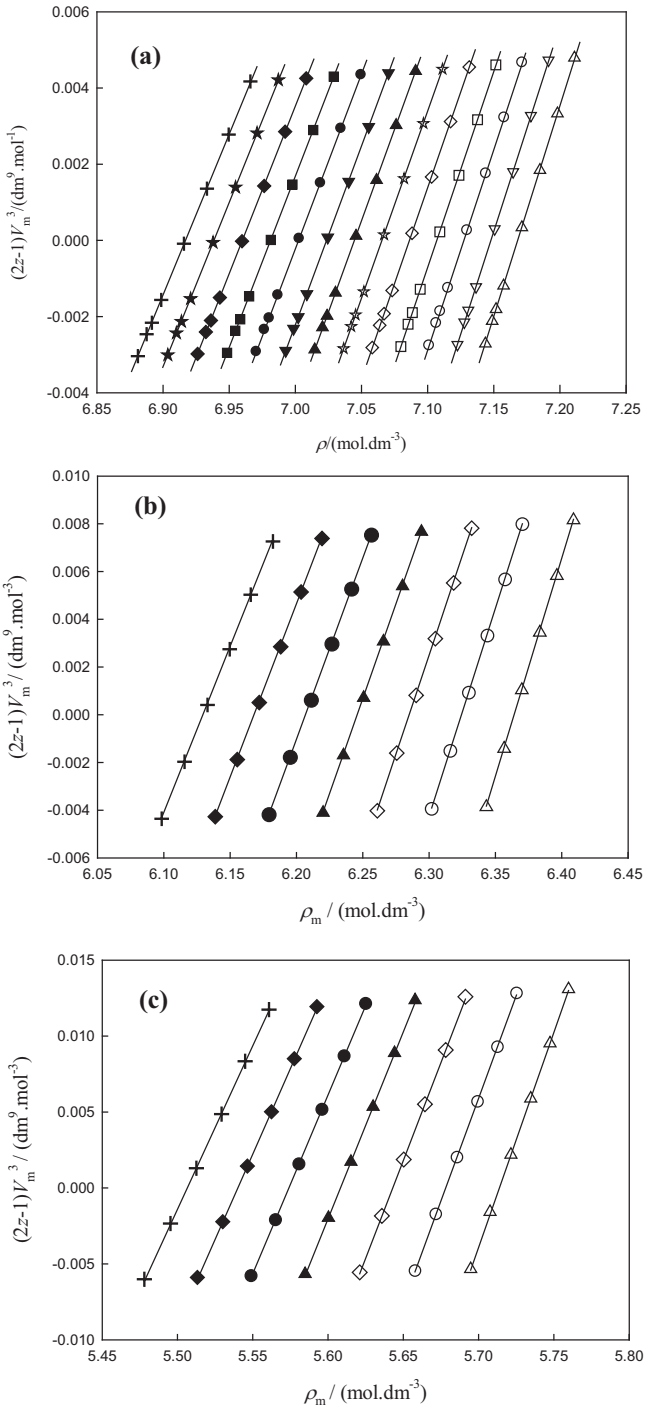

FIGURE 4. Isotherms of $(2z-1)V_m^3$ versus ρ_m for the *N*-methyl-2-hydroxyethylammonium carboxylic ILs: (a) $[C_{2OH}C_1NH_2][C_2COO]$; (b) $[C_2OHC_1NH_2][C_3COO]$; (c) $[C_2OHC_1NH_2][C_4COO]$. Legend as in figure 2.

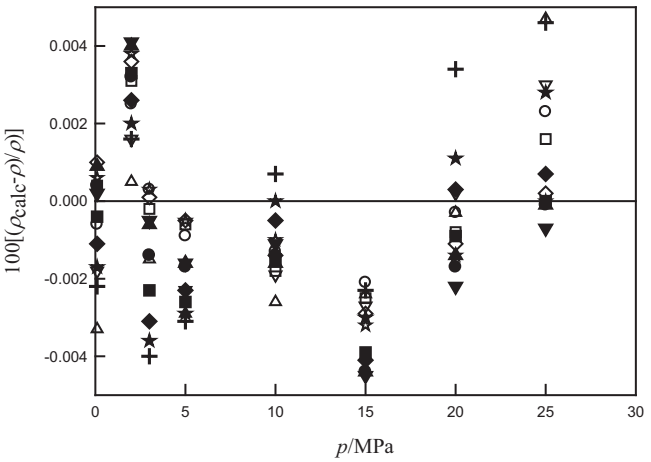

FIGURE 5. Relative density deviations between the calculated values with GMA EoS (ρ_{calc}) and the experimental values (ρ) for $[C_2OHC_1NH_2][C_2COO]$. Legend as in figure 2(a).

where ρ is the density in kg · m^{-3}, M is the IL molar mass in kg ·mol^{-1}, N is the Avogadro number, V is the molecular volume in m^3, T is the temperature in K, and p is the pressure in MPa. The coefficients a, b and c were previously proposed [51]: a = 0.8005, b = 6.652 · 10^{-4} - K^{-1} and c = -5.919 · 10^{-4} MPa^{-1}. The molecular volumes of the protic ILs obtained by the fitting of equation (11) to the experimental density data are listed in table 3 where the *AAD*% between fitted and experimental densities is also presented. It can be seen that the differences in the molecular volumes in adjacent ILs are 2.97 nm^3 and this value can be mostly attributed to the inclusion of (–CH_2–) group by assuming that $V = V^+ + V^-$. In this way, V(–CH_2–) = 2.97 nm^3 which is in good agreement with the value of V(–CH_2–) = 2.80 nm^3 given by Costa *et al.* [64]. Gardas and Coutinho obtained a molecular volume of $V(CH_3COO^-)$ = 8.55 nm^3 for the acetate anion by structural considerations [51]. Considering V(–CH_2–) = 2.97 nm^3 the ionic molecular volumes listed in table 3 were obtained. A constant value of V $[C_2OHC_1NH_2]^+$ = 11.75 nm^3 was obtained for the common cation. On the other hand Neves *et al.* [65] obtained V $[C_9COO^-]$ = 2.90 nm^3 for the decanoate anion. By considering $V(C_1COO^-)$ = 8.55 nm^3 for the acetate anion and that

$$V[C_9COO^- = 2.90\ nm^3] = V[C_1COO^- = 8.55\ nm^3] + 8V(-CH_2-),$$

we obtain V(–CH_2–) = 2.56 nm^3 a value that is in good agreement with the value given by Ye and Shreeve [63]. With this contribution for the methylene group, the ionic molecular volumes listed in parenthesis in table 3 were found. In table 3, the ionic molecular volumes calculated from equation (11) for *N*-methyl-2 hydroxyethylammonium formate ($[C_2OHC_1NH_2][HCOO]$) and for *N*-methyl-2 hydroxyethylammonium acetate ($[C_2OHC_1NH_2][C_1COO]$) are also given using the experimental density data from Àlvarez *et al.* [46] in the range T = (278.15 to 335.16) K at atmospheric pressure. It is observed that the value V ($[C_2OHC_1NH_2][C_1COO]$ = 20.31 nm^3) = V ($[C_2OHC_1NH_2][C_2COO]$) = 23.28 nm^3) – 2.97 nm^3 is similar to the one obtained directly from equation (11). On the other hand V $[C_1COO]^-$ = V ($[C_2OHC_1NH_2][C_1COO]$ = 20.40) – 11.75] = 8.65 nm^3 is obtained in close agreement with the value found by Gardas and Coutinho from structural considerations. From the value $V[C_2OHC_1NH_2][HCOO]$ = 17.83 nm^3 no values of molecular volumes for the formate anion for purpose of comparison were found in the open literature. We estimate $V[HCOO]^-$ = V($[C_2OHC_1NH_2]$ [HCOO] = 17.83) – 11.75] = 6.08 nm^3.

The method of Paduszyńki and Domańska [52] has been recently proposed and is a group contribution method based in the Tait equation, in which the molar volume at reference temperature (298.15 K) and pressure (0.1 MPa) was assumed to be additive with respect to a defined set of both cationic and anionic functional groups. It was developed based on a database containing over 18,500 data points for a variety of 1028 ILs. The collected data cover temperature and pressure ranges of T = (253 to 473) K and p = (0.1 to 300) MPa, respectively. The model parameters, including contributions to molar volume for 177 functional groups, as well as universal coefficients describing the *PVT* surface, were fitted to experimental data for 828 ILs with AAD% = 0.53%. The model was applied to 200 ILs not included in the correlation set with a resulting AAD% = 0.45%. The density of the IL at reference temperature

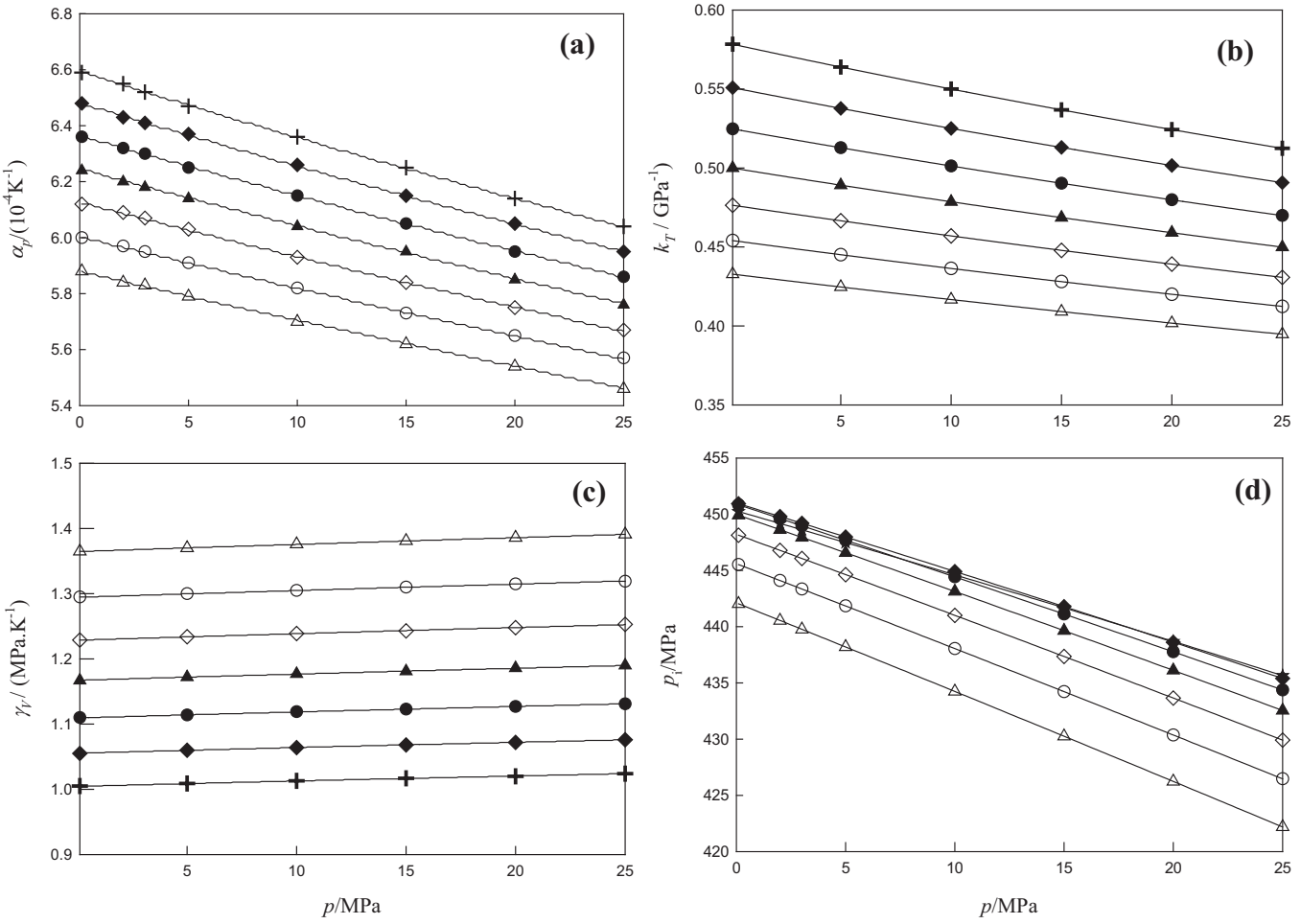

FIGURE 6. Thermal expansivity, α_p, isothermal compressibility, k_T; thermal pressure γ_V and internal pressure p_i for the *N*-methyl-2-hydroxyethylammonium carboxylic ILs calculated from GMA EoS equation as a function of the pressure and the temperature: (a) $[C_2OHC_1NH_2][C_2COO]$; (b) $[C_2OHC_1NH_2][C_3COO]$; (c) $[C_2OHC_1NH_2][C_4COO]$; (d) $[C_2OHC_1NH_2][C_2COO]$. Legend: experimental data of this work: Δ, T = 298.15 K; ○, 308.15 K; ◇, 318.15 K; ▲, 328.15 K; ●, 338.15 K; ♦, 348.15 K; +, 358.15 K. Full curves calculated from GMA EoS equation.

TABLE 3
Values of molecular volumes of ionic species of N-methyl-2-hydroxyethylammonium carboxylic PILs.

Ionic liquid	V/nm	V^+/nm	V^-/nm	σ/kg · m^{-3}	AAD/%[b]
$[C_2OHC_1NH_2][HCOO]$	17.83	11.75	6.08	3.6	0.27
$[C_2OHC_1NH_2][C_1COO]$	20.40	11.75	8.55[a]	2.3	0.18
$[C_2OHC_1NH_2][C_2COO]$	23.28	11.76 (12.17)	11.52 (11.11)	1.8	0.13
$[C_2OHC_1NH_2][C_3COO]$	26.24	11.75 (12.58)	14.49 (13.66)	1.2	0.10
$[C_2OHC_1NH_2][C_4COO]$	29.21	11.75 (12.99)	17.46 (16.22)	1.1	0.09

[a] value taken as starting point for calculations.
[b] AAD % between fitted equation (11) to the experimental densities.

and pressure conditions $\rho_0 = \rho$ (T_0 = 298.15 K, p_0 = 0.1 MPa) is given by the following formula

$$\rho_0 = \rho(T_0, p_0) = \frac{M}{V_{0,m}}, \tag{12}$$

where M is the molar mass of the IL and $V_{0,m}$ denotes molar volume at (T_0, p_0) which is calculated based on the GCM additivity principle:

$$V_{0,m} = \sum_i n_i \, v_i^0. \tag{13}$$

Symbols n_i and v_i^0 correspond to the number of occurrences of functional group of type i and the contribution of that group to molar volume at (T_0, p_0). By adopting equation (13), the "ideal" behaviour of the ILs reported by Rebelo *et al.* [66] and also observed by Canongia Lopes *et al.* [67] is assumed. This means that both cation and anion effective volumes of a given ion are independent of any counter ions composing the IL system. In this model, a linear relationship between molar volume and temperature at reference pressure, namely

$$\rho(T, p_0) = \frac{M}{V_{0,m}[1 + 6.439 \cdot 10^{-4}(T - T_0)]} = \frac{\rho_0}{1 + 6.439 \cdot 10^{-4}(T - T_0)}, \tag{14}$$

is combined with the a Tait-type equation for compressed fluid:

$$\rho(T, p) = \frac{\rho(T, p_0)}{1 - 0.081 \ln[1 + B(T)(p - p_0)]}, \tag{15}$$

TABLE 4
Group assignments and the results of calculations for (PD) model for PVT of the N-methyl-2-hydroxyethylammonium carboxylic PILs. The numbers of occurrences of groups in each PIL (n_i) and assigned groups are as given by Paduszyński and Domańska [52]. (AAD %) is the Average Absolute Deviation for estimated density.

Ionic liquid	Group assignment			$10^6 \sum_i n_i v_i^0$/cm^3 · mol^{-1}[b]	AAD/%
$[C_2OHC_1NH_2][HCOO]$[a]	$n_{41}=1;\ n_{106}=1;\ n_{117}=1;n_{125}=1;\ n_{159}=1;\ n_{160}=1$			110.30	2.7
$[C_2OHC_1NH_2][C_1COO]$[a]	$n_{41}=1;\ n_{103}=1;\ n_{117}=1;n_{125}=1;\ n_{159}=1;\ n_{160}=1$			123.14	0.3
$[C_2OHC_1NH_2][C_2COO]$	$n_{41}=1;\ n_{104}=1;\ n_{116}=1;\ n_{117}=1;n_{125}=1;\ n_{159}=1;n_{160}=1$			143.63	2.7
$[C_2OHC_1NH_2][C_3COO]$	$n_{41}=1;\ n_{104}=1;\ n_{116}=1;\ n_{117}=2;n_{125}=1;\ n_{159}=1;n_{160}=1$			160.36	1.9
$[C_2OHC_1NH_2][C_4COO]$	$n_{41}=1;\ n_{104}=1;\ n_{116}=1;\ n_{117}=3;n_{125}=1;\ n_{159}=1;n_{160}=1$			177.09	1.1
	List of functional groups present in the PILs[b]				
41. $[NH_2]^+$		$v_i^0 = 23.04$	117. CH_2	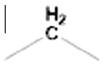	$v_i^0 = 16.73$
103. $[CH_3COO]^-$	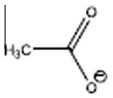	$v_i^0 = 52.00$	125. OH	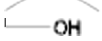	$v_i^0 = 9.077$
104. $[CH_2COO]^-$	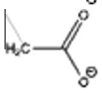	$v_i^0 = 46.33$	159. N–CH_3	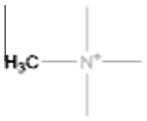	$v_i^0 = 15.79$
106. $[HCOO]^-$	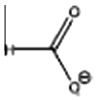	$v_i^0 = 39.20$	160. N–CH_2	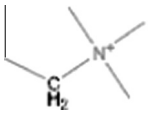	$v_i^0 = 6.5$
116. CH_3		$v_i^0 = 26.16$			

[a] Comparison with data from Álvarez *et al.* [46] at $T = 298.15$ K and $p = 0.1$ MPa.
[b] v_i^0/m^3 · mol^{-1}.

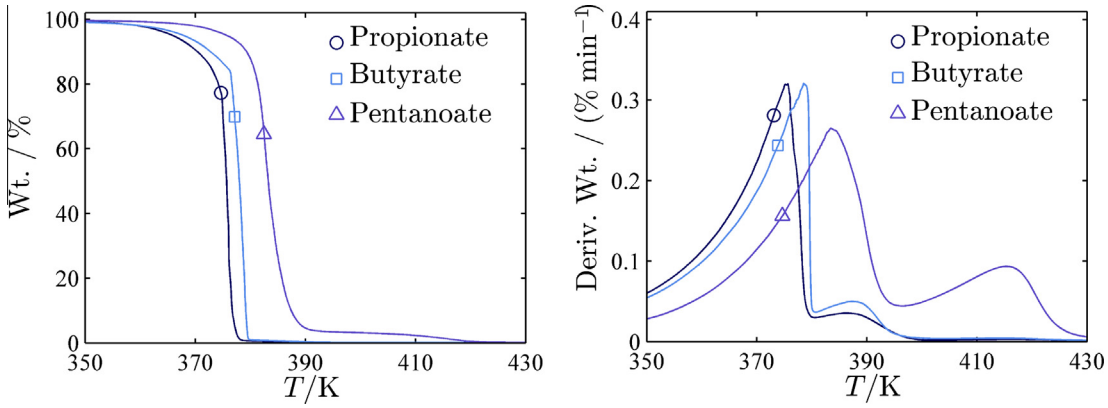

FIGURE 7. Thermogravimetric curves (left) and respective time derivatives (right) of the N-methyl-2-hydroxyethylammonium IL samples by HRMTGA (amplitude of modulation: ±5 K; period of modulation 200 s) at 2 K · min^{-1}.

where

$$B(T) = \frac{1}{195}\left[1 + 4.97 \cdot 10^{-3}(T - T_0)\right]. \quad (16)$$

The results of application of the PD model to the PILs of this work are presented in table 4. The group assignments for all ILs (*i.e.*, the values of n_i) and the group contributions are also tabulated. Some ILs with 2-hydroxyethylammonium cation with various carboxylic acid anions were considered in the model. The densities of ammonium cations collected in the database by Paduszyński and Domańska containing the hydroxyethyl group (–C_2OH) and at the same time paired with carboxylic anions, include 2-hydroxyethylammonium (or $[C_2OHNH_3]^+$), bis(2-hydroxyethyl)ammonium (or $[(C_2OH)_2NH_2]^+$), and tris(2-hydroxyethyl)ammonium (or $[(C_2OH)_3NH]^+$) and formate, acetate, and pentanoate anions. The only cation with methyl group included in the large database of the authors was bis(2-hydroxyethyl)(methyl)ammonium (or $[(C_2OH)_2C_1NH]^+$) coupled with acetate anion. The densities of these ILs were studied over a 60 K range near the ambient temperature and at $p = 0.1$ MPa and they are predicted by the PD model with average absolute relative deviations ranging from 0.2% to 2.5%, *i.e.*, the density deviations are similar to those found for the N-methyl-2-hydroxyethylammonium ILs studied in this work in the given ranges of pressure and temperature.

3.2. Thermal stability

An evaluation of the thermal stability of the PILs prior to the study of their thermophysical properties is highly desirable, if not mandatory. The thermal stability study was investigated by HiResMTGA. Figure 7 includes both the TGA curves and their derivative counterparts, and table 5 summarizes data selected from the thermoanalytical curves. The main features demonstrated by these results can be summarized as follow.

The overall thermal degradation profiles of the analyzed ILs are similar. They are characterized by a slow mass loss rate at the

TABLE 5
Characteristic quantities obtained from HRMTGA curves (2 K · min^{-1}; amplitude of modulation: ±5 K; period of modulation 200 s). T_{on}: extrapolated onset temperature; $T_{n\%}$: temperature at n% mass loss; T_p: peak temperature(s) (DTG curves).

IL	T_{on}/K	$T_{2\%}$/K	$T_{5\%}$/K	$T_{10\%}$/K	T_{p1}/K	T_{p2}/K
$[C_2OHC_1NH_2][C_2COO]$	342.5	334.4	335.0	344.9	350.7	361.2
$[C_2OHC_1NH_2][C_3COO]$	343.5	340.8	342.8	351.6	353.5	362.3
$[C_2OHC_1NH_2][C_4COO]$	353.6	345.3	347.7	355.1	360.0	391.3

beginning of the decomposition process, which starts at $T_{1\%}$ (temperature at 1% mass loss) of *ca.* (327, 326 and 337) K, respectively for $[C_2OHC_1NH_2][C_2COO]$, $[C_2OHC_1NH_2][C_3COO]$, and $[C_2OHC_1NH_2][C_4COO]$, followed by a sharp mass loss stage (more evident in propionate and butyrate), the latter corresponding to *ca.* 80% of the total decomposition. Both propionate and butyrate are essentially completely decomposed along with that abrupt mass loss stage, whereas pentanoate exhibits a residual mass (*ca.* 3.4% at T = 373 K) whose decomposition is essentially completed at *ca.* 403 K.

The thermal stability of the ILs (based on the indexes T_{on}, $T_{2\%}$, $T_{5\%}$, $T_{10\%}$, and T_{p1}; see figure 7 and table 5) increases in the order $[C_2OHC_1NH_2][C_2COO] < [C_2OHC_1NH_2][C_3COO] << [C_2OHC_1NH_2][C_4COO]$. This trend appears to be a manifestation of the role of the carboxylic acid anions in the thermal stability, suggesting an enhanced thermal stability as the size of that moiety increases.

Finally, it is of interest to notice that the thermal stability of the N-methyl-2-hydroxyethylammonium based ionic liquids reported here is significantly lower than those of a series of quaternary phosphonium-based ILs liquids recently studied [68] under similar experimental conditions. The thermal stability of N-methyl-2-hydroxyethylammonium ILs of this study are also lower than the values found in the literature for 2-hydroxyethylammonium ILs with carboxylic anions [41,69]. For 2-hydroxyethylammonium formate, $[C_2OHNH_3][HCOO]$, Bicak [69] found that TGA curve shows a sharp decline around T = 423 K and an inflection at about 463 K, and that 100% mass losses occur at 550 K. The analysis was made in a Shimadzu TG-50 at 10 K · min^{-1} heating rate, under nitrogen flow, 23 cm^3 · min^{-1}. For 2-hydroxyethylammonium acetate $[C_2OHNH_3][CCOO]$, Kurnia *et al.* [41] gives T_d = 558.52 K, $T_{10\%} \approx$ 433 K, and at *ca.* 573 K, 100% mass losses occur. These authors used a different thermogravimetric analyzer (TGA, Perkin Elmer, Pyris V-3.81) with different operating conditions (Platinum pan under N_2 atmosphere, at a heating rate of 10 K · min^{-1}). Although the comparisons made before involve cations which differ by one methyl group and anions with small different alkyl chain extension it remains valid. The differences can be attributed in part to the different heating and flow rates. Higher heating rates shift TGA curves to the right giving higher decomposition temperatures.

3.3. Heat capacity

In a recent paper, we have presented heat capacities for phophonium based ILs measured by modulated differential scanning calorimetry (MDSC) [68]. Differential scanning calorimeters (DSCs) and modulated DSC (MDSC) have an uncertainty of at least 5% but the uncertainties of the data obtained with calorimeters of the same model in different laboratories may vary considerably. The experimental results obtained in this work are reported in tables S5 to S8 (supplementary material) and are plotted in figure 8. For each IL, several series of measurements were made and it is observed that for each IL all the series are consistent with each other in the measured ranges of temperature. For $[C_2OHC_1NH_2][C_3COO]$, there is a difference between the two series by about 2% (*ca.* 9 J · K^{-1} · mol^{-1}) at the higher temperatures. The heat capacity increases in the order $[C_2OHC_1NH_2][C_2COO] < [C_2OHC_1NH_2][C_3COO] < [C_2OHC_1NH_2][C_4COO]$. The experimental values of heat capacity are arranged in almost parallel lines which result from the methylene group (–CH_2–) contribution in the anion (*ca.* 37 J · K^{-1} · mol^{-1} at T = 298.15 K). This value is the same as that found in our previous study with phosphonium ILs [68] and is rather higher than the value given in the group contribution method developed by Rùzicka and Domalski for calculation of molecular liquid heat capacities [70]. Gardas and Coutinho [54] propose a value of 31.98 J · K^{-1} · mol^{-1} while Valderrama *et al.* [57] give an increment of 31.51 J · K^{-1} · mol^{-1}, in good agreement with that experimentally reported by Rocha *et al.* [71], to be used in their group contribution method for aprotic ionic liquids.

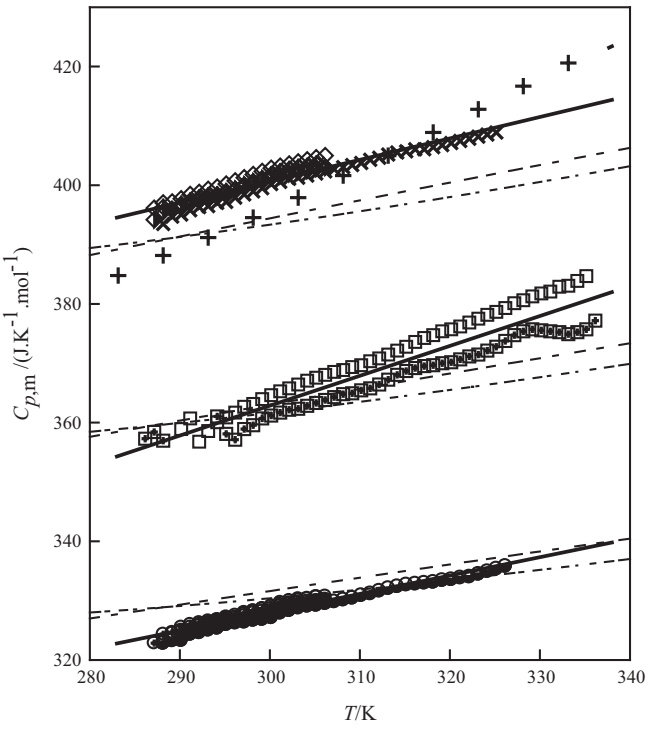

FIGURE 8. Molar heat capacity of PILs as a function of temperature. $[C_2OHC_1NH_2][C_2COO]$; ○, series 1; ⊙, series; , series 3; ◑, series 4; ◒, series 5. $[C_2OHC_1NH_2][C_3COO]$: □ series 1, ⊡, series 2. $[C_2OHC_1NH_2][C_4COO]$, sample1: ◇, series 1; ⟡, series 2; ◈, series 3; × series 4. $[C_2OHC_1NH_2][C_4COO]$: +, Sample2. The solid lines refer to equation (17). The lines (——) and (–·–) refer to the prediction by Ge *et al.* [73] and Valderrama *et al.* [57] methods, respectively.

To describe the dependency of heat capacity on temperature, the function

$$C_{p,m} = c_0 + c_1 T \qquad (17)$$

was used, where c_0 and c_1 are correlation coefficients to be obtained by least square fitting to the molar heat capacity data. Table 6 summarizes the temperature range of heat capacity measurements, $T = (T_{min}$ to $T_{max})$, the coefficients c_0 and c_1, the standard deviation, σ, correlation coefficient, R, the AAD%, and the number of data points, N_p, used in the fittings. The AAD% is defined as in equation (6) using here the molar heat capacity as the property under comparison. The experimental heat capacity obtained at T = 298.15 K, $C_{p,298}$ is also given in table 6. The relative deviations between the calculated heat capacity by equation (17) and experimental for the different series of measurements are presented in figure 9. The relative deviations are usually in ±0.5% corresponding to ±2 J · K^{-1} · mol^{-1} at the higher heat capacity measured.

TABLE 6
Fitting parameters of equation (17), temperature range of experimental data (T_{min}, T_{max}), molar heat capacity at T = 298.15 K, statistical characteristics of individual data sets for the fit (Standard deviation, σ, absolute average deviation, *AAD%*, correlation coefficient, R), and number of points used in the fit, N_p.

Parameter	$[C_2OHC_1NH_2][C_2COO]$	$[C_2OHC_1NH_2][C_3COO]$	$[C_2OHC_1NH_2][C_4COO]$
c_0/(J · K^{-1} · mol^{-1})	235.31 ± 2.09	211.74 ± 6.27	292.46 ± 3.56, 181.36 ± 2.93[a]
c_1/(J · K^{-2} · mol^{-1})	0.3091 ± 0.0069	0.5037 ± 0.0200	0.3607 ± 0.0118, 0.7161 ± 0.095[a]
T_{min}/K	287.15	286.15	287.15, 283.15[a]
T_{max}/K	326.15	336.15	325.15, 333.15[a]
$C_{p,298}$ /(J · K^{-1} · mol^{-1})	327.7 ± 0.6	361.4 ± 1.8	400.5 ± 1.0, 394.9[a]
σ/(J · K^{-1} · mol^{-1})	0.7	2.6	1.1, 0.5[a]
R	0.974	0.936	0.953, 0.999[a]
AAD/%	0.17	0.65	0.22, 0.10[a]
N_p	111	92	96, 11[a]

[a] Values found for sample 2.

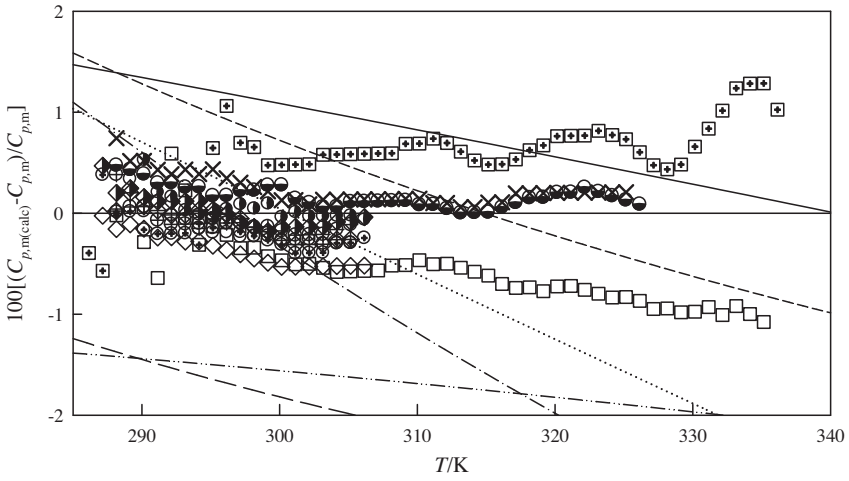

FIGURE 9. Relative deviations between calculated heat capacity $C_{p,m(calc)}$, and the measured values from this work, $C_{p,m}$. Symbols refer to the calculated values with equation (17) (legend as in figure 8). The lines refer to the values calculated with Ge *et al.* and by Valderrama *et al.* methods, respectively. $[C_2OHC_1NH_2][C_2COO]$, (- - - -), (——); $[C_2OHC_1NH_2][C_3COO]$, (—·—), (····); $[C_2OHC_1NH_2][C_4COO]$, (— —), (—··—··).

The heat capacities of several N-alkyl-(2-hydroxyethyl)-ammonium ILs are compared in figure 10 where measurements for alkyl-(2-hydroxyethyl)-dimethylammonium bromide [48], for alkyl-(2-hydroxyethyl)-ammonium sulphonates and sulphates [49], and the PILs studied here are presented. The values for alkyl-(2-hydroxyethyl)-dimethylammonium bromides measured by Domanska and Bogel-Lucasik [48] are somewhat unexpected because the heat capacity of propyl-(2-hydroxyethyl)-dimethylammonium bromide is almost the same as for butyl-(2-hydroxyethyl)-dimethylammonium bromide. However the values for hexyl-(2-hydroxyethyl)-dimethylammonium bromide are close to the expected considering the methylene group increment. The values of molar heat capacity measured by Maharova *et al.* [49] for N-ethyl-N-(2-hydroxyethyl)-N,N-dimethylammonium methylsulphonate, are of the same order of magnitude as our measured values for N-(2-hydroxyethyl)-N-methylammonium butyrate and pentanoate extrapolated to higher temperatures. The heat capacity of N-ethyl-N-(2-hydroxyethyl)-N,N-dimethylammonium octanesulfonate is high compared to methylsulfonate mainly because to the seven methylene groups in the alkyl chain attached to the sulfonate anion. For N-(2-hydroxyethyl)-N,N,N-trymethylammonium bis(trifluoromethylsulfonyl)imide, $[C_2OH(C_1)_3N][NTf_2]$, Nockemann *et al.* [72] obtained $C_{p,m}$ = 417.4 J · K^{-1} · mol^{-1} at T = 303.15 K, by an indirect method. This value is not far from the $C_{p,m}$ here reported for 2-hydroxyethyl-N-methylammonium pentanoate which contains cationic and anionic structures different from $[C_2OH(C_1)_3N][NTf_2]$.

Two predictive methods for the estimation of molar heat capacities of liquids were applied. The Joback method for ideal gas heat capacity with subsequent use of the principle of corresponding states to calculate the liquid heat capacity was used. In this calculation, the modified Lydersen–Joback–Reid method developed by Valderrama and Rojas [55] is applied to calculate the critical properties of ILs. The complete procedure is described in detail by Ge *et al.* [73]. The Valderrama *et al.* [57] mass connectivity index method was also applied. In this the method the molar heat capacity as a function of the temperature is calculated by

$$C_{p,m}(T) = \sum_i g_i G_i + 9.0045 - 100.70\lambda + \lambda(0.3918T - 1.952 \cdot 10^{-4}T^2), \quad (18)$$

where g_i and G_i are the number frequency and the contribution value of group i, respectively. The mass connectivity index λ is defined as

$$\lambda = \sum \left(\frac{1}{(m_i m_j)^{1/2}}\right)_{ij}, \quad (19)$$

where m_i and m_j are the mass of neighbouring groups i and j in a molecule. In summing up the connections, $m_i m_j$ is considered different of $m_j m_i$ so that a "bond" between groups i and j is considered twice in the calculation of λ. In table 7, the relevant parameters for the application of the methods of prediction are given. The heat capacity found in this work for N-methyl-2-hydroxyethylammonium propionate, butyrate and pentanoate is compared with the predicted heat capacities by the predictive methods in figure 8. The predictions can be considered as acceptable, although the experimental temperature dependency of the heat capacities is

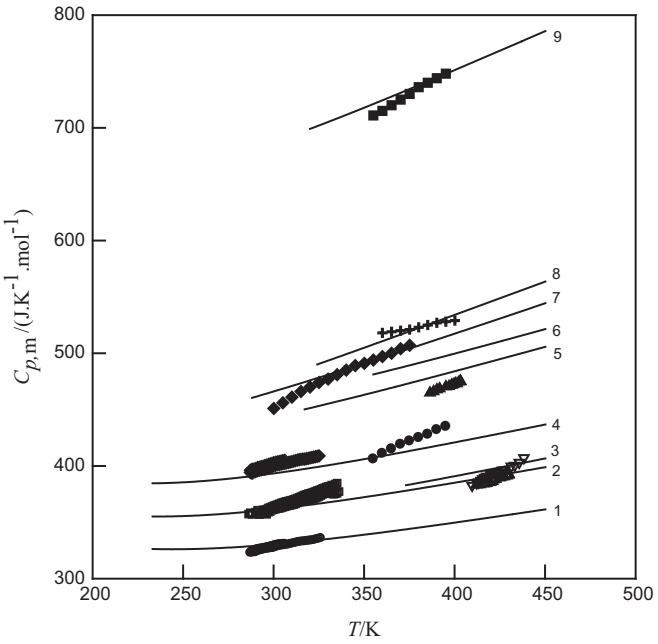

FIGURE 10. Molar heat capacity of alkyl-(2-hydroxyethyl)-ammonium ILs as a function of temperature. Experimental data: - This work, ○, [$C_2OHC_1NH_2$][C_2COO]; □, [$C_2OHC_1NH_2$][C_3COO]; ◇, [$C_2OHC_1NH_2$][C_2COO]. Literature: Δ, [$C_2OHC_3(C_1)_2$N][Br] [48]; , [$C_2OHC_4(C_1)_2$N][Br] [48]; ●, [C_2OH (C_2)(C)$_2$N][C_1SO_3], [49]; ▲, [C_2OHC_6(C1)$_2$N][Br] [48]; ♦, [$C_2OH(C_2)(C)_2$N][C_2SO_4], [49]; +, [$C_2OH(C_3)$N][C_4SO_3], [49]; ■, [$C_2OH(C_2)(C)_2$N][C_8SO_3], [49]. Prediction with Ge *et al.* method: 1, [$C_2OHC_1NH_2$][C_2COO]; 2, [$C_2OHC_1NH_2$][C_3COO]; 3, [$C_2OHC_3(C)_2$N][Br]; 4, [$C_2OHC_1NH_2$][C_4COO]; 5, [$C_2OH(C_2)(C)_2$N][C_1SO_3]; 6, [C_2OHC_6(C1)$_2$N][Br]; 7, [$C_2OH(C_2)(C)_2$N][C_2SO_4]; 8, [$C_2OH(C)_3$N][C_4SO_3]; 9, [$C_2OH(C_2)(C)_2$N][C_8SO_3].

significantly higher than the predicted. In figure 10 the experimental and the predicted (T, $C_{p,m}$) behaviour from the Ge *et al.* method is compared for the several N-alkyl-(2-hydroxyethyl)-ammonium PILs. As observed previously for our data, the predictions are consistent with the measured values with the exceptions of the data for N-hexyl-(2-hydroxyethyl)-dimethylammonium bromide and N-ethyl-(2-hydroxyethyl)-dimethylammonium methanesulfonate. In table 7, a detailed quantitative comparison between predicted and experimental values is presented for all the alkyl-(2-hydroxyethyl)-ammonium PILs. In figure 9, the relative deviations between predicted and experimental heat capacities are presented for the PILs considered in this work. The experimental values were represented by equation (17). We conclude that for the PILs studied here, the heat capacity values predicted from both methods are similar and are in agreement with the experimental values. For alkyl-(2-hydroxyethyl)-ammonium other than those of this work, the results from Valderrama *et al.* method were not presented in figure 10 and in table 7 because the predicted values of heat capacity are very low when compared to the experimental ones. This discrepancy is mainly due to the (very) low heat capacity contribution given in the methodology for the quaternary ammonium group with substitution in all the four positions. It should be noted at this point that the mothod of Valderrama *et al.* was developed using 469 data points for 32 ILs and 126 data for 126 organic compounds and that the only ammonium considered was the tetrabutylammonium docusate [57]. Concerning the discrepancies between measured and predicted heat capacity for N-hexyl-(2-hydroxyethyl)-dimethylammonium bromide and N-ethyl-(2-hydroxyethyl)-dimethylammonium methanesulfonate, two aspects must be mentioned. Firstly, considering the –CH_2- increments (≈37 J · K^{-1} · mol^{-1}) and the experimental heat capacity values given for N-propyl-(2-hydroxyethyl)-dimethylammonium bromide [48], one can obtain values close to those predicted with the method of Ge *et al.* for N-hexyl-(2-hydroxyethyl)-dimethylammonium bromide. Second, taking the experimental data for N-ethyl-(2-hydroxyethyl)-dimethylammonium octanesulfonate [49] and subtracting the methylene contribution, values close to those predicted with the method of Ge *et al.* are obtained for N-ethyl-(2-hydroxyethyl)-dimethylammonium methanesulfonate. These results suggest that the measurements for those ILs are probably not very accurate.

TABLE 7
Parameters for the prediction methods of heat capacity for N-methyl-2-hydroxyethylammonium carboxylic PILs of this work and other from the literature.

Ionic liquid	T_b[a] (K)	T_c[a] (K)	P_c[a] (MPa)	V_c[a] (cm^3 · mol^{-1})	ω[a]	λ	$C_{p,m}$[b]/(J · K^{-1} · mol^{-1})			$C_{p,m}/V_m$[c] (J · K^{-1} · cm^{-3})
							Exp	Ge	Vald	
[$C_2OHC_1NH_2$][C_2COO]	499.7	676.5	3.41	453.6	0.86	0.828	328(298)	330	331	2.34
							351(350)	339	343	2.38
							359 (400)	350	353	2.41
[$C_2OHC_1NH_2$][C_3COO]	522.6	698.8	3.06	510.7	0.90	0.970	361 (298)	361	363	2.30
							388 (350)	372	376	2.38
							413 (400)	385	388	2.46
[$C_2OHC_1NH_2$][C_4COO]	545.5	721.1	2.78	567.8	0.93	1.113	401(298)	393	394	2.34
							419 (350)	406	409	2.38
							437 (400)	421	423	2.41
[$C_2OHC_3(C_1)_2$N][Br]	531.9	710.1	2.74	569.3	0.85		376 (400)	390		1.96
[$C_2OHC_6(C_1)_2$N][Br]	600.6	776.6	2.16	740.7	0.96		444 (350)	479		1.93
							473 (400)	500		
[$C_2OH(C_1)_3$N][C_4SO_3]	499.7	677.0	1.38	1113.8	0.38		514 (350)	505		2.40
							529 (400)	534		2.39
[$C_2OHC_2(C_1)_2$N][C_1SO_3]	870.5	1212.0	1.53	999.6	0.29		404 (350)	463		2.05
							439 (400)	484		2.16
[$C_2OHC_2(C_1)_2$N][C_8SO_3]	1030.6	1322.9	1.13	1399.3	0.59		706 (350)	718		2.22
							754 (400)	751		2.30
[$C_2OHC_2(C_1)_2$N][C_2SO_4]	499.7	683.0	1.46	1072.3	0.36		491 (350)	491		2.21
							516 (400)	517		2.30
[$C_2OH(C_1)_3$N][NTf_2]	761.7	1073.8	3.08	862.0	0.56		417 (303)	596		1.70

[a] Calculated with the modified Lydersen–Joback–Reid method developed by Valderrama and Rojas [55].
[b] The experimental values $C_{p,exp}$ were calculated from the linear equation (17). For the N-alkyl-(2-hydroxyethyl)-dimethylammonium ILs studied by Domanska and Bogel-Lucasik [48] and the ones by Maharova *et al.* [49] the coefficients are given as supplementary material in table S9.
[c] As the studies made by Domanska and Bogel-Lucasik [48] and by Maharova *et al.* [49] do not provide the density, the molar volume was calculated from Paduszyński and Domańska model. The molar volume $V_{0,m} = V$ (T_0 = 298.15 K, p_0 = 101.325 kPa) is given in table S9.

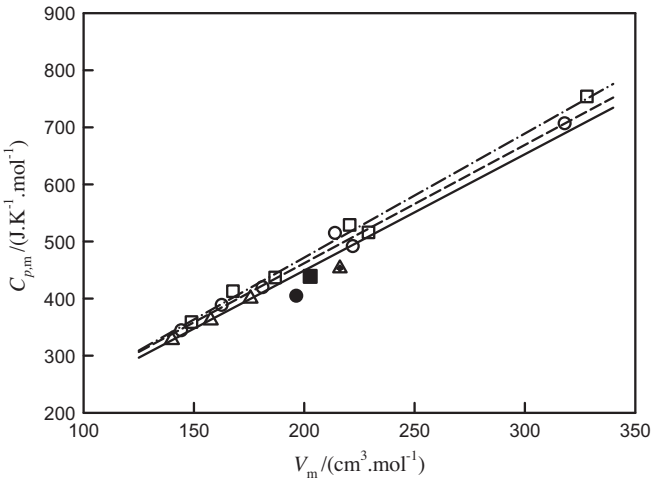

FIGURE 11. Molar heat capacity of alkyl-(2-hydroxyethyl)-ammonium ILs as a function of molar volume. Δ, T = 298.15 K; ○, T = 350.15 K; □, T = 400.15 K. The lines refer to the linear fitting: (——). T = 298.15 K; (---) T = 350.15 K; (—·—) T = 400.15 K. Outliers: ◭, $[C_2OH(C_2)(C)_2N][C_2SO_4]$ at T = 298.15 K; ●, $[C_2OH(C_2)(C)_2N][C_1SO_3]$ at T = 350.15 K; ■, $[C_2OH(C_2)(C)_2N][C_1SO_4]$ at T = 400.15 K.

Simple linear correlations of the molar heat capacity with the molar volume have been proposed for ILs at T = 298.15 K [54,74,75]. From experimental heat capacity and molar volumes given in table 7 at temperatures T = (298, 350, and 400) K, we obtain good linear ($C_{p,m}$, V_m) correlations at isothermal conditions for the alkyl-(2-hydroxyethyl)-ammoniums ILs, as displayed in Figure 11. The exceptions are the N-ethyl-N-(2-hydroxyethyl)-N,N-dimethylammonium methanesulfonate at T = (350 and 400) K and the N-ethyl-N-(2-hydroxyethyl)-N,N-dimethylammonium ethylsulfate at 298.15 K. The equation

$$C_{p,m}/(\mathrm{J\cdot K^{-1}\cdot mol^{-1}}) = -31.11 + 0.1985\,(T/\mathrm{K}) + 2.1201\,(V_m/\mathrm{cm^3\cdot mol^{-1}}), \quad (20)$$

describes the experimental values of all the N-alkyl-(2-hydroxyethyl)ammonium ILs within a standard error σ = ±12 J · mol^{-1} · K^{-1}, AAD% = 1.7%, and the maximum relative deviation of -4.0%.

The heat capacity to molar volume ratio ($C_{p,m}/V_m$) is an important parameter in the evaluation of effective application of ILs as heat accumulators. From a set of 19 aprotic ILs, Gardas and Coutinho [54] first suggested this value to be (1.95 ± 0.01) J · K^{-1} · cm^{-3} at T = 298.15 K. Later Paulechka *et al.* [75] showed that this ratio ($C_{p,m}/V_m$) varied with temperature between values of (1.95 ± 0.02) J · K^{-1} · cm^{-3} at 298.15 K and (2.00 ± 0.02) J · K^{-1} · cm^{-3} at 350 K. The data set used by these authors included only one ammonium IL [C_3 $(C_1)_3N$][NTf_2]. From table 7, it is observed that while for the alkyl-(2-hydroxyethyl)-ammoniums ILs considered in this study, the ($C_{p,m}/V_m$) values are significantly higher than the values found for aprotic ionic liquids this quotient is nevertheless very similar for the PILs studied on this work. The very high molar heat capacity to molar volume quotient of alkyl-(2-hydroxyethyl)-ammoniums ILs (2.0 to 2.4) make this family of ILs interesting for several thermal applications including heat capacity storage. Therefore in a future work the determination of transport properties such as, thermal conductivity, and viscosity will be object of study.

4. Conclusions

Experimental density data for N-methyl-2-hydroxyethylammonium cation with propionate, butyrate and pentanoate anions are presented over the ranges of temperature and pressure, respectively T = (298.15 to 358.15) K and p = (0.1 to 25) MPa, with an estimated uncertainty of ±0.5 kg · m^{-3}. The GMA EoS reproduces accurately the experimental (p T) values of the PILs studied with deviations in the range 0.005% which means less than 0.1 kg · m^{-3}. The (p, T) behaviour of k_T calculated from the GMA EoS are in general consistent with those experimentally observed. The minimum values are of the order 0.4 MPa^{-1}, the maximum values are in the range (0.5 to 0.6) MPa^{-1}. The values of k_T increase in the order $[C_2OHC_1NH_2][C_2COO] < [C_2OHC_1NH_2][C_3COO] < [C_2OHC_1NH_2][C_4COO]$. The behaviour of α_p is somewhat erratic in the sense that it behaves accordingly to the observed behaviour for $[C_2OHC_1NH_2][C_2COO]$ but shows little variation for $[C_2OHC_1NH_2][C_3COO]$ and $[C_2OHC_1NH_2][C_4COO]$. The minimum values of α_p are of the order (5.5 to 6) · 10^{-4} K^{-1}, being the maximum *ca.* 6.6 · 10^{-4} K^{-1}. The internal pressure shows small changes for each PIL and it increases in the order $[C_2OHC_1NH_2][C_2COO] > [C_2OHC_1NH_2][C_3COO] > [C_2OHC_1NH_2][C_4COO]$, reaching its minimum value of p_i = 340 MPa for $[C_2OHC_1NH_2][C_4COO]$ (at T = 358 K, p = 25 MPa) while at the same (p,T) conditions p_i = 436 MPa for $[C_2OHC_1NH_2][C_2COO]$. The isothermal decrease with pressure is always observed and the temperature is variable with the nature of PIL. This situation is due to the small range of variation of γ_V with temperature and pressure.

High resolution modulated thermogravimetric analysis indicated the following relative stabilities for the studied PILs: $[C_2OHC_1NH_2][C_2COO] < [C_2OHC_1NH_2][C_3COO] << [C_2OHC_1NH_2][C_4COO]$. This trend appears to be controlled by the carboxylic acid anions being thermal stability enhanced as the size of that moiety increases. The thermal stability of N-methyl-2-hydroxyethylammonium ILs of this study is lower compared with what is reported in the literature for 2-hydroxyethylammonium ILs with carboxylic anions. This issue deserves further investigation because the thermal stability depends on the operating conditions used during the TGA analysis.

Modulated differential scanning calorimetry (MDSC) allowed the measurement of the heat capacities of the ILs within a temperature interval T = (286 to 336) K, with a mean uncertainty of 5 J · K^{-1} · mol^{-1}. The heat capacity increases in the order $[C_2OHC_1NH_2][C_2COO] < [C_2OHC_1NH_2][C_3COO] < [C_2OHC_1NH_2][C_4COO]$, and the ($T$, $C_{p,m}$) are arranged in almost parallel lines due to the methylene group (–CH_2–) contribution in the anion (*ca.* 37 J · K^{-1} · mol^{-1} at 298.15 K). The (T, $C_{p,m}$) for the PILs studied are well correlated by linear functions. Taking the experimental values of (T, V_m, $C_{p,m}$) for ten alkyl-(2-hydroxyethyl)-ammonium PILs, a new correlation linear in the temperature and in the molar volume is proposed allowing the prediction of heat capacity of alkyl-(2-hydroxyethyl)-ammoniums ILs with uncertainties of the order of 12 J · K^{-1} · mol^{-1}. This uncertainty is lower than differences sometimes found in measured heat capacities for a given IL by different authors.

Acknowledgments

The authors are grateful to UE Mobility Programme which supported the Grant (EADIC II – ERASMUS MUNDUS ACTION 2 LOT 13A UE Mobility Programme 2010-2401/001-001 – EMA2) and to the Fundação para a Ciência e a Tecnologia which funded CICECO through Pest-C/CTM/LA0011/2011. S. Mattedi is grateful to CNPq (Project 475883/2012-8) and UFBA (Project PROPI/2013) for funding her work. The authors acknowledge the support from Eng. Paula V. Egas for her assistance in the ILs management.

Appendix A. Supplementary data

Supplementary data associated with this article can be found, in the online version, at http://dx.doi.org/10.1016/j.jct.2013.09.010.

References

[1] T. Ramnial, D.D. Ino, J.A.C. Clyburne, Chem. Commun. (2005) 325–327.
[2] A.J. Arduengo, Acc. Chem. Res. 32 (1999) 913–921.
[3] S.A. Chowdhury, J.L. Scott, D.R. MacFarlane, Pure Appl. Chem. 80 (2008) 1325–1335.
[4] C. Yao, W.R. Pitner, J.L. Anderson, Anal. Chem. 81 (2009) 5054–5063.
[5] P. Scovazzo, D. Camper, J. Kieft, J. Poshusta, C. Koval, R. Noble, Ind. Eng. Chem. Res. 43 (2004) 6855–6860.
[6] M.B. Shiflett, A. Yokozeki, AIChE J. 52 (2006) 3952–3957.
[7] B. Wu, R.G. Reddy, R.D. Rogers, Solar Energy: The Power to Choose, April 21–25, 2001, Proc. Solar Forum, 2001, Washington, DC, 2001.
[8] K.-S. Kim, B.-K. Shin, H. Lee, F. Ziegler, Ionic, liquids as new working fluids for use in absorption heat pumps or chillers: their thermodynamic properties, in: 15th Symposium on Thermophysical Properties, Colorado Univ, Colorado, June, 2003. 23–27.
[9] P. Scovazzo, A.E. Visser, J.H. Davis Jr., R.D. Rogers, C.A. Koval, D.L. DuBois, R.D. Noble, ACS Symp. Ser. 818 (2002) 69–87.
[10] L. Weng, X.Q. Liu, Y.M. Liang, Q.J. Xue, Tribol. Lett. 26 (2007) 11–17.
[11] J. Qu, J.J. Truhan, S. Dai, H. Luo, P.J. Blau, Tribol. Lett. 22 (2006) 207–214.
[12] K. Tsunashima, M. Sugiya, Electrochem. Commun. 9 (2007) 2353–2358.
[13] D.H. Zaitsau, G.J. Kabo, A.A. Strechan, Y.U. Paulechka, A. Tschersich, S.P. Verevkin, A. Heintz, J. Phys. Chem. A 110 (2006) 7303–7306.
[14] D.F. Kennedy, C.J. Drummond, J. Phys. Chem. B 113 (2009) 5690.
[15] J. Pernak, I. Goc, I. Mirska, Green Chem. 6 (2004) 323–329.
[16] R.V. Hangarge, D.V. Jarikote, M.S. Shingare, Green Chem. 4 (2002) 266–268.
[17] K.K. Laali, V.J. Gettwert, J. Org. Chem. 66 (2001) 35–40.
[18] Y. Hu, J. Chen, Z.G. Le, Q.G. Zheng, Synth. Commun. 35 (2005) 739–744.
[19] C.F. Poole, J. Chromatogr. A 1037 (2004) 49–82.
[20] M.A.B.H. Susan, A. Noda, S. Mitsushima, M. Watanabe, Chem. Commun. 8 (2003) 938–939.
[21] M.J. Earle, N.V. Plechkova, K.R. Seddon, Pure Appl. Chem. 81 (2009) 2045–2057.
[22] J.C. Galvez-Ruiz, G. Holl, K. Karaghiosoff, T.M. Klapotke, K. Lohnwitz, P. Mayer, H. Noth, K. Polborn, C.J. Rohbogner, M. Suter, J.J. Weigand, Inorg. Chem. 44 (2005) 4237–4253.
[23] M. Picquet, I. Tkatchenko, I. Tommasi, P. Wasserscheid, J. Zimmermann, J. Adv. Synth. Catal. 345 (2003) 959–962.
[24] S. Gabriel, Berichte 21 (1888) 2664–2669.
[25] P. Walden, Bull. Acad. Imp. Sci. (1914) 1800–1801.
[26] D.F. Evans, S.H. Chen, G.W. Schriver, E.M. Arnett, J. Am. Chem. Soc. 103 (1981) 481–482.
[27] D.F. Evans, A. Yamauchi, G.J. Wei, V.A. Bloomfield, J. Phys. Chem. 87 (1983) 3537–3541.
[28] D.F. Evans, E.W. Kaler, W.J. Benton, J. Phys. Chem. 87 (1983) 533–535.
[29] D.F. Evans, Langmuir 4 (1988) 3.
[30] D.F. Evans, A. Yamauchi, R. Roman, E.Z. Casassa, Colloid Interface Sci. 88 (1982) 89–96.
[31] A.H. Beesley, D.F. Evans, J. Phys. Chem. 92 (1988) 791–793.
[32] R.B. Trusler, Ind. Eng. Chem. 21 (1929) 685–687.
[33] S. Zhu, M. Heppenstall-Butler, M.F. Butler, P.D.A. Pudney, D. Ferdinando, K.J. Mutch, J. Phys. Chem. B 109 (2005) 11753–11761.
[34] S. Zhu, P.D.A. Pudney, M. Heppenstall-Butler, M.F. Butler, D. Ferdinando, M. Kirkland, J. Phys. Chem. B 111 (2007) 1016–1024.
[35] P.D.A. Pudney, K.J. Mutch, S.P. Zhu, Phys. Chem. Chem. Phys. 11 (2009) 5010–5018.
[36] H. Alvarez, S. Mattedi, M. Martin-Pastor, M. Aznar, M. Iglesias, Fluid Phase Equilib. 299 (2010) 42–50.
[37] N.E. Meyer, Am. J. Surg. 40 (1938) 628–629.
[38] K. Yamamoto, H. Sakaguchi, H. Anai, T. Tanaka, K. Morimoto, K. Kichikawa, H. Uchida, Cardiovascular Intervent. Radiol. 28 (2005) 751–755.
[39] M.G. Kiripolsky, Dermatol. Surg. 36 (2010) 1153–1154.
[40] C.C. Gomes, R.S. Gomez, M.A. do Carmo, W.H. Castro, A. Gala-Garcia, R.A. Mesquita, Medicina oral, patologia oral y cirugia bucal 11 (2006) E44–46.
[41] K.A. Kurnia, C.D. Wilfred, T. Murugesan, J. Chem. Thermodyn. 41 (2009) 517–521.
[42] M. Iglesias, R. Gonzalez-Olmos, I. Cota, F. Medina, J. Chem. Eng. Data 162 (2010) 802–808.
[43] J. Sierra, E. Marti, A. Mengibar, R. Gonzalez-Olmos, M. Iglesias, R. Cruañas, M.A. Garau, Effect of new ammonium based ionic liquids on soil microbial activity, in: 5th Society of Environmental Toxiology and Chemistry Word Congress, August 3–7, Sydney, Australia, 2008.
[44] T.L. Greaves, A. Weerawardena, C. Fong, I. Krodkiewska, C.J. Drummond, J. Phys. Chem. B 110 (2006) 22479–22487.
[45] J.P. Belieres, C.A. Angell, J. Phys. Chem. B 111 (2007) 4926–4937.
[46] V.H. Álvarez, N. Dosil, R. Gonzalez-Cabaleiro, S. Mattedi, M. Martin-Pastor, M. Iglesias, J.M. Navaza, J. Chem. Eng. Data 55 (2010) 625–632.
[47] A. Pinkert, K.L. Ang, K.N. Marsh, S. Pang, Phys. Chem. Chem. Phys. 13 (2011) 5136–5143.
[48] U. Domanska, R. Bogel-Łukasik, J. Phys. Chem. B 109 (2005) 12124–12132.
[49] M. Mahrova, M. Vilas, A. Domínguez, E. Gómez, N. Calvar, E. Tojo, J. Chem. Eng. Data 57 (2012) 241–248.
[50] E.K. Goharshadi, A. Morsali, M. Abbaspour, Fluid Phase Equilib. 230 (2005) 170–175.
[51] R. Gardas, J. Coutinho, Fluid Phase Equilib. 263 (2008) 26–32.
[52] K. Paduszynki, U. Domanska, Ind. Eng. Chem. Res. 51 (2012) 591–604.
[53] J.A.P. Coutinho, Pedro J. Carvalho, Nuno M.C. Oliveira, RSC Adv. 2 (2012) 7322–7346.
[54] Ramesh L. Gardas, João A.P. Coutinho, Ind. Eng. Chem. Res. 47 (2008) 5751–5757.
[55] J.O. Valderrama, R.E. Rojas, Ind. Eng. Chem. Res. 48 (2009) 6890–6900.
[56] J.O. Valderrama, R.E. Rojas, Fluid Phase Equilib. 297 (2010) 107–112.
[57] J.O. Valderrama, A. Toro, R.E. Rojas, J. Chem. Thermodyn. 43 (2011) 1068–1073.
[58] V.G. Niesen, J. Chem. Thermodyn. 21 (1989) 915–923.
[59] R.L. Gardas, I. Johnson, D.M.D. Vaz, I.M.A. Fonseca, A.G.M. Ferreira, J. Chem. Eng. Data 52 (2007) 737–751.
[60] Fluid properties for water, http://webbook.nist.gov/chemistry/fluid/ (July 2013).
[61] F.A.M.M. Gonçalves, C.S.M.F. Costa, J.C.S. Bernardo, I. Johnson, I.M.A. Fonseca, A.G.M. Ferreira, J. Chem. Thermodyn. 43 (2011) 105–116.
[62] F.A.M.M. Gonçalves, C.S.M.F. Costa, C.E. Ferreira, J.S. Bernardo, I. Johnson, I.M.A. Fonseca, A.G.M. Ferreira, J. Chem. Thermodyn. 43 (2011) 914–929.
[63] C. Ye, J.M. Shreeve, J. Phys. Chem A 111 (2007) 1456–1461.
[64] A.J.L. Costa, J.M.S.S. Esperança, I.M. Marrucho, L.P.-N. Rebelo, J. Chem. Eng. Data 56 (2011) 3433–3441.
[65] C.M.S.S. Neves, P.J. Carvalho, M.G. Freire, J.A.P. Coutinho, J. Chem. Thermodyn. 43 (2011) 948–957.
[66] L. Rebelo, J. Canongia Lopes, J. Esperanca, H. Guedes, J. Yachwa, V. Najdanovic-Visak, Z. Visak, Acc. Chem. Res. 40 (2007) 1114–1121.
[67] J. Canongia Lopes, T. Cordeiro, J. Esperanca, H. Guedes, S. Huq, L.P. Rebelo, K.J. Seddon, Phys. Chem. B 109 (2005) 3519–3525.
[68] A.F. Ferreira, P.N. Simões, A.G.M. Ferreira, J. Chem. Thermodyn. 45 (2012) 16–27.
[69] N. Bicak, J. Mol. Liquids 116 (2005) 15–18.
[70] V. Rùzicka, E.S. Domalski, J. Phys. Chem. Ref. Data 22 (1993) 619–658.
[71] M.A.A. Rocha, M.B.J.A.P. Coutinho, L.M.N.B.F. Santos, J. Chem. Thermodyn. 53 (2012) 140–143.
[72] P. Nockemann, K. Binnemans, B. Thijs, T.N. Parac-Vogt, K. Merz, A.V. Mudring, P.C. Menon, R.N. Rajesh, G. Cordoyiannis, J. Thoen, J. Leys, C. Glorieux, J. Phys. Chem. B 113 (2009) 1429–1437.
[73] R. Ge, C. Hardacre, J. Jacquemin, P. Nancarrow, D.W. Rooney, J. Chem. Eng. Data 53 (2008) 2148–2153.
[74] A.A. Strechan, A.G. Kabo, Y.U. Paulechka, A.V. Blokhin, G.J. Kabo, A.S. Shaplov, E.I. Lozinskaya, Thermochim. Acta 474 (2008) 25–31.
[75] Y.U. Paulechka, A.G. Kabo, A.V. Blokhin, G.J. Kabo, M.P. Shevelyova, J. Chem. Eng. Data 55 (2010) 2719–2724.

JCT 13-514